THEORETICAL MODELLING FOR HELICOPTER FLIGHT DYNAMICS: DEVELOPMENT AND VALIDATION

G.D. Padfield
Flight Dynamics Division,
Royal Aerospace Establishment, Bedford, UK

ICAS-88-6.1.3

SUMMARY

A fully validated and accurate mathematical model of the helicopter offers the potential to explore new concepts in a timely fashion at the research and feasibility stage, conduct vehicle and control system design with confidence and reduce certification timescales through the extended use of piloted simulation. Striving to achieve this potential is a worthy objective, not only on economic grounds, but also because more efficient and balanced designs have such a strong and positive impact on flight safety. This paper argues that although this tenet may be generally accepted, a number of factors have hindered flight dynamics modelling in the feasibility to certification life cycle of many helicopter projects. The lack of precise and substantial design criteria, the immaturity of rational validation techniques and the limitation of processing power are three such factors but the sheer aeromechanical complexity has presented the greatest intellectual challenge. This paper describes this complexity in terms of two fundamental dimensions, frequency and amplitude or bandwidth and nonlinearity. While a detailed aeroelastic formulation may be necessary to describe and predict some phenomena, reduced order model structures are adequate for others. To gain maximum physical insight into flight behaviour, the simplest adequate model is the most useful. The paper looks at different modelling levels required to predict lateral, directional, longitudinal and vertical axis dynamics; techniques of system identification are used to compare flight test results with theoretical predictions. The measurement set required to validate aeroelastic models is also discussed and example results presented.

1 INTRODUCTION

The majority of current operational helicopters, in both civil and military service, have experienced considerable delays during development and certification, while problems, not predicted in the design phases, have had to be cured. Such problems cover a wide range of helicopter technologies but those relating to flying qualities and flight control are particularly demanding on flight time and highly skilled human resources. Also, the impact of deficiencies in these areas on flight safety is a strong motivation to seek a permanent and complete cure, although experience has shown that this is very difficult to achieve and a reduced operational envelope is often a practical compromise. The single most important contribution to this class of problems has been the deficiency in the predictive capability of the design simulation model. This may appear a rather obvious conclusion but the solution has been greatly hindered by the lack of substantial design criteria on the one hand and a rational modelling validation methodology on the other. Mandatory, and even advisory, design criteria for flying qualities have been so ill-matched to the modern high performance helicopter that achieving compliance has provided virtually no insight into the problems that may arise. Validation has been based on ad-hoc techniques, drawn from a sparse database, and often left until the aircraft is built and flying before being taken seriously as an activity. While the situation is unsatisfactory, it is understandable in view of the difficult technical challenges involved. Three developments underway will offer a mechanism for improving the situation. Firstly the emergence of new, more structured and demanding design criteria will provide the designer with practical goals, more appropriate to modern day operations. Secondly, the growth in maturity of system identification methods for application to helicopters will provide a more rational and systematic framework for validation. Thirdly, computer analysis tools for optimisation and simulation are becoming easier to integrate into the design process through faster processing and user-friendly interfaces.

While these three 'initiatives' will provide support in the design-certification life cycle, substantial improvements will come only with improvements in the accuracy of predictive modelling, eg under exactly what conditions will components break, closed loops go unstable or control limits be reached. Achieving the appropriate level of modelling for flight control design is a major challenge here. Further motivation comes from the pressure to conduct full mission simulation with high modelling fidelity throughout and beyond the operational flight envelope. The natural dimensions are frequency range and nonlinearity and, with the introduction of high gain active control into helicopters, both go beyond levels normally associated with human pilot operation. This paper is concerned with these natural modelling dimensions and approaches the subject from a framework of the related UK RAE research programme.

Early helicopter simulation research at RAE[1] demonstrated that basic modelling methods were adequate for providing the pilot with the correct response cues for 'gentle flying'. Later, prompted by the growing interest in helicopter agility, a new generic model (Helisim)[2] was developed and successfully employed to establish key vehicle and control system design parameters that affected handling in agile flight[3]. Validation studies, conducted through simple analogue response matching with flight test data, highlighted a number of modelling deficiencies for this kind of flying, however, even though parametric trends were broadly correct. To determine if an improved model data set would be adequate, or whether a development of the model structure was necessary, a more systematic approach to validation was required. A research activity into system identification for helicopters was initiated at RAE and a suite of analysis tools developed to support interpretive validation[4,5]. This research has guided modelling improvements over the last few years, through measures of

predictive accuracy and checks on modelling assumptions. Validation as an activity is closely linked with measurement requirements, ie there has to be compatibility between the level of model detail and the experimental measurements used in validation. In recognition of this, parallel developments in the sensor/instrumentation fit to the flight research helicopters at RAE and the test techniques and experimental design have taken place.

This paper draws on results from RAE research into model development and validation to highlight the natural model dimensions and stress the compatibility of model complexity and measurement set. Chapter 2 discusses in more detail the elements of flight mechanics model structures and the need for an integrated approach to system identification for helicopters. Chapter 3 presents examples from 6 degree of freedom 'classical' linear analysis and higher order modelling while Chapter 4 discusses the requirements for aeroelastic modelling. Chapter 5 completes the paper with a summary of the principal results and recommendations for future initiatives.

2 MODEL DEVELOPMENT AND VALIDATION METHODS

2.1 Model structures

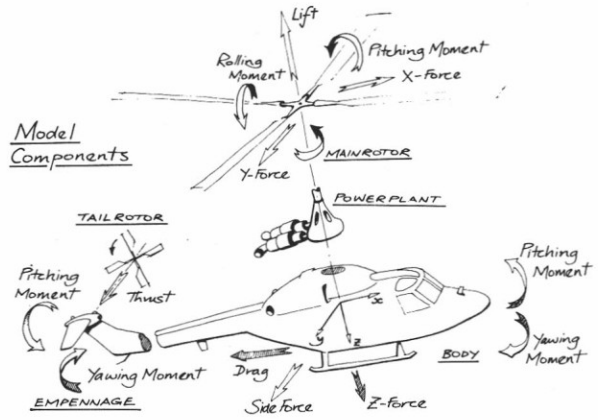

Fig 1 Helicopter model components

In mathematical terms, the helicopter represents a complex arrangement of interacting sub-systems that can be viewed from a component (Fig 1) or dynamics perspective; the former based on a breakdown into physical parts, eg main rotor, fuselage etc, the latter based on a partitioning into physical or mathematical sub-systems arranged and interconnected according to their frequency and amplitude content. The second is a more convenient framework for discussion in this paper and it is further convenient to partition the model structure into three levels, differentiated largely by the form of rotor modelling, as summarised in Table 1. Level 1 modelling includes the 'rigid body', six degree of freedom linear or nonlinear formulation with quasi-steady rotor dynamics and extends to the inclusion of rotor blade dynamics in multi-blade coordinate forms[6] with analytically integrated blade loadings, together with a range of additional dynamic elements, eg engine/rotorspeed, actuators etc. Aerodynamic inflow representation in Level 1 modelling extends from the uniform 'momentum' concept with a linear variation longitudinally across the disc, to dynamic inflow[2,6]. Such models are useful for flying qualities and performance studies within the normal flight envelope where integrated rotor loads are not significantly affected by rotor stall, compressibility effects and the attendant rotor blade dynamic couplings. They provide the basis for practically all of the piloted simulation research conducted to date. Level 3 modelling, at the other extreme, represents the most comprehensive rotor/fuselage modelling necessary to predict, not only integrated, but also vibratory loadings across a wide frequency bandwidth. This is, in general, unnecessarily complex to be appropriate to flight mechanics work. Nevertheless, increased exploitable primary flight control bandwidth, and flight in conditions where aerodynamic nonlinearities and rotor couplings prevail, require modelling enhancements for piloted simulation. The complexity required for this modelling is still an area of research and Table 1 suggests possible elements, under the Level 2 heading.

The behaviour of a rotor blade under aerodynamic load is determined by the geometric, inertial and elastic properties and one of the keys to efficient Level 2 modelling will be the determination of the simplest adequate model description. For Level 1 models, on the other hand, gross simplifications are traditional and a simple pin

Table 1

LEVELS OF HELICOPTER THEORETICAL MODEL

	Level 1	Level 2	Level 3
Aerodynamics	Linear 2-D Dynamic inflow/local momentum theory Analytically integrated loads	Nonlinear (limited 3-D) Dynamic inflow/local momentum theory Local effects of blade/vortex interaction Unsteady 2-D Compressibility Numerically integrated loads	Nonlinear (3-D) Full wake analysis (free or prescribed) Unsteady 2-D Compressibility Numerically integrated loads
Dynamics	(i) Rigid blades 6 d.o.f. quasi-steady rotor 9 d.o.f.—rotor flapping 12 d.o.f.—flap + lag 15 d.o.f.—flap + lag + pitch	(i) Rigid blades Options as in Level 1 (ii) Limited number of blade elastic modes	(i) Elastic modes (detailed structural) representation
Application	Parametric trends for flying qualities/performance studies Within operational flight envelope Low bandwidth control	Parametric trends for flying qualities/performance studies Beyond operational flight envelope Medium bandwidth appropriate to high gain active flight control	Rotor design Rotor load prediction across a high bandwidth Beyond operational flight envelope

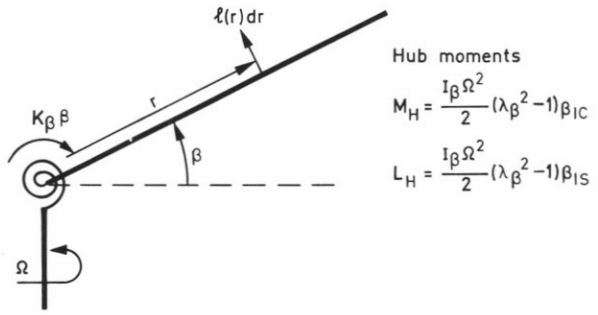

Fig 2 Centre-spring rotor model

jointed, spring restrained rigid blade is the basis of most flap modelling. The most rudimentary form has the hinge at the centre of rotation (Fig 2) and satisfies the approximate equation,

$$\beta'' + \lambda_\beta^2 \beta = \frac{2}{\Omega}(p \cos\psi - q \sin\psi) + \gamma \int_0^1 \ell(r,\psi) r dr \qquad (1)$$

where β is the blade flap angle, p and q the fuselage roll and pitch rates and $\ell(r,\psi)$, the normalised aerodynamic loading along the normalised radial dimension r. ψ is the blade azimuth angle and $\beta' = d\beta/d\psi$; $\psi = \Omega t$, where Ω is the rotor speed. λ_β and γ are the flapping frequency ratio and Lock number respectively, given by

$$\lambda_\beta^2 = 1 + \frac{K_\beta}{I_\beta \Omega^2} \qquad (2)$$

$$\gamma = \frac{\rho c a_o R^4}{I_\beta} \qquad (3)$$

where K_β is the spring strength, I_β the blade 2nd moment of inertia, ρ the air density, c and R the blade chord and radius respectively and a_o the blade lift curve slope. These two fundamental scaling parameters can be matched, for the centre spring analogue, to equivalent parameters associated with either hinged or hingeless rotors, in the case of the latter derived from the first elastic mode natural frequency and modal inertia. Typical values for λ_β range from unity for teetering to 1.1 for hingeless rotors; γ represents a ratio of aerodynamic to inertia effects and can vary between 6 and 12.

Equation (1) reveals that blade flapping motion conforms to simple harmonic motion with the centrifugal and spring stiffening, resulting in blade flapping response being close to 90° out-of-phase with once/rev aerodynamic inputs, eg cyclic pitch. This phase resonance effect is the key to understanding rotor dynamics and has led to the common description in terms of harmonics or multi-blade coordinates[2,6]. Transforming equation (1) into the first three harmonic components of flap, and reducing to first-order form, leads to the 'tip-path-plane' equation,

$$\dot{\underset{\sim}{\beta}}_m - A_\beta \underset{\sim}{\beta}_m = \underset{\sim}{h}_\beta (\underset{\sim}{x}_f , \underset{\sim}{\theta}_m , \underset{\sim}{\lambda}_m) \qquad (4)$$

where $\underset{\sim}{\beta}_m = [\beta_o , \beta_{1c} , \beta_{1s}]^T$,

$\underset{\sim}{x}_f = [u , w , q , \theta , v , p , \phi , r]^T$,

$\underset{\sim}{\theta}_m = [\theta_o , \theta_{1c} , \theta_{1s}]^T$ and

$\underset{\sim}{\lambda}_m = [\lambda_o , \lambda_{1c} , \lambda_{1c}]^T$.

Subscripts 0 , 1c , 1s denote zeroth, first cosine and first sine components of flap (β_m) , blade pitch (θ_m) and induced downwash (λ_m) respectively. $\underset{\sim}{x}_f$ is the vector of fuselage dynamic motions with translational velocities (u , v , w) and rotational velocities (p , q , r) about the usual body axes system rotated through Euler angles θ and ϕ relative to earth. The matrix A_β and vector $\underset{\sim}{h}_\beta$ are, in general, functions of flight state and rotor azimuth ψ ; however, in the transformation to tip-path-plane coordinates the lowest harmonics appearing here are n/rev, where n is the number of blades. A further approximation involves neglecting these terms, leaving equation (4) as a dominant constant coefficient first order system. Assuming autonomous downwash dynamics and rigid body fuselage motions, the coupled linearised system can be written in the form

$$\frac{d}{dt}\begin{bmatrix} \underset{\sim}{x}_f \\ \underset{\sim}{\beta}_m \\ \underset{\sim}{\lambda}_m \end{bmatrix} - \begin{bmatrix} A_f & A_{f\beta} & A_{f\lambda} \\ A_{\beta f} & A_\beta & A_{\beta\lambda} \\ A_{\lambda f} & A_{\lambda\beta} & A_\lambda \end{bmatrix} \begin{bmatrix} \underset{\sim}{x}_f \\ \underset{\sim}{\beta}_m \\ \underset{\sim}{\lambda}_m \end{bmatrix} = \begin{bmatrix} B_{fu} \\ B_{\beta u} \\ B_{\lambda u} \end{bmatrix} \underset{\sim}{u} \qquad (5)$$

The generalised control vector $\underset{\sim}{u}$ and associated B matrices can include control motivators (eg tail rotor, tailplane etc) in addition to the main rotor controls $\underset{\sim}{\theta}_m$. Along with other discrete elements representing lag dynamics, actuator dynamics, engine/rotorspeed dynamics etc, equation (5) represents a general form of stationary system, or Level 1, modelling for rotorcraft. The model structure can be truncated using reduced order modelling concepts[7,8], and allow, for example, the conventional 6 degree of freedom approximation to be realised. From equation (5), this takes the form,

$$\dot{\underset{\sim}{x}}_f - \left[A_f - \begin{bmatrix} A_{f\beta} & A_{f\lambda} \end{bmatrix} \begin{bmatrix} A_\beta & A_{\beta\lambda} \\ A_{\lambda\beta} & A_\lambda \end{bmatrix}^{-1} \begin{bmatrix} A_{\beta f} \\ A_{\lambda f} \end{bmatrix} \right] \underset{\sim}{x}_f$$

$$= \left[B_{fu} - \begin{bmatrix} A_{f\beta} & A_{f\lambda} \end{bmatrix} \begin{bmatrix} A_\beta & A_{\beta\lambda} \\ A_{\lambda\beta} & A_\lambda \end{bmatrix}^{-1} \begin{bmatrix} B_{\beta u} \\ B_{\lambda u} \end{bmatrix} \right] \underset{\sim}{u} \quad . \qquad (6)$$

Implicit in this linearised version of the 6 degree of freedom helicopter model is the usual approximation of retaining only the first terms in a series expansion of external loads about the trim point. Thus, from equation (6), aerodynamic derivatives can be written as a sum of partial derivatives from the 'higher order' contributions; eg, for the incidence stability derivative, M_w, we can write,

$$M_w = \frac{\partial M}{\partial w} + \frac{\partial M}{\partial \beta_{1c}} \frac{\partial \beta_{1c}}{\partial w} + \frac{\partial M}{\partial \lambda_o} \frac{\partial \lambda_o}{\partial w} + \ldots \qquad (7)$$

Typical of Level 1 modelling is the RAE Helisim[2] real-time model and the interactive development version HELISTAB. Fig 3 illustrates the general

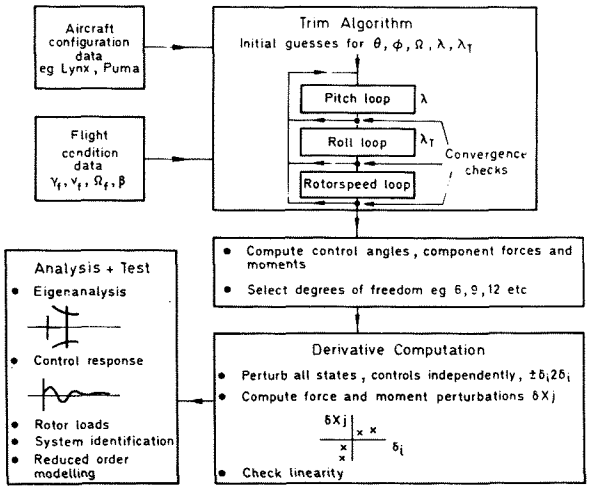

Fig 3 Structure of Helistab flight mechanics analysis

structure and facilities within this latter software package.

2.2 System identification

Validation of the adequacy of a given model structure to predict loads and dynamic behaviour needs to be based on comparison with test data and the tools of system identification have been developed to provide a rational mechanism for the derivation of model structure and parameter estimates from test data. A number of features peculiar to helicopters combine to make the application of system identification difficult. These include system complexity, high vibration environment, potentially strong nonlinearities and instabilities and air data measurements sensitive to rotor wake and fuselage flowfield effects. An integrated approach needs to be adopted as shown

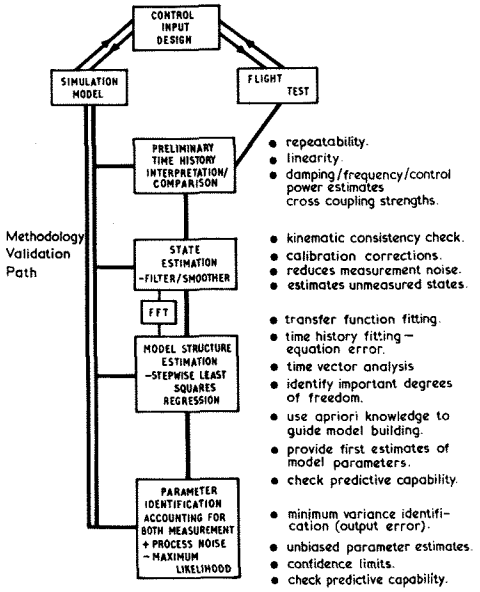

Fig 4 Integrated system identification methodology

in Fig 4, ranging from test input design through kinematic compatibility checks to model structure and parameter estimation. A software package developed in the UK[4,5] through a joint RAE/Glasgow University research programme provides these facilities as a research tool, and results from this analysis will be used in Chapter 3 of this paper. Both equation-error and output-error methods are used, the former based on the computationally efficient least-squares regression algorithm, the latter on maximum-likelihood minimisation. With a system of the form,

$$\dot{\underset{\sim}{x}} = \underset{\sim}{f}(\underset{\sim}{x}, \underset{\sim}{\delta}) \qquad (8)$$

where $\underset{\sim}{\delta}$ is a vector of unknown parameters within a functional form $\underset{\sim}{f}(\underset{\sim}{x}, \underset{\sim}{\delta})$ of unknown structure. Model Structure Estimation (MSE) has the goal of establishing the best form of the latter in terms of the degrees of freedom $\underset{\sim}{x}$; initial estimates for $\underset{\sim}{\delta}$ are also derived at this stage and are required as starting values for the output-error iterations. MSE requires an equation-error formulation, ie,

$$\dot{\underset{\sim}{x}}_m - \underset{\sim}{f}(\underset{\sim}{x}_m, \underset{\sim}{\delta}) = \underset{\sim}{\varepsilon} \; ; \; \min_{\underset{\sim}{\delta}} \underset{\sim}{g}_e(\underset{\sim}{\varepsilon}) \qquad (9)$$

$\underset{\sim}{g}_e(\underset{\sim}{\varepsilon})$ is some function of the error function $\underset{\sim}{\varepsilon}$ (eg mean square). The regression algorithm is simple to implement but requires measurements of all states $(\underset{\sim}{x}_m)$ and their derivatives $(\dot{\underset{\sim}{x}}_m)$, and gives biased estimates in the presence of

measurement noise. Output-error analysis, on the other hand, only requires measurements of system states, ie,

$$\underset{\sim}{x}_m - \int_o^t \underset{\sim}{f}(\underset{\sim}{x}_m , \underset{\sim}{\delta})dt = \underset{\sim}{\varepsilon} \quad ; \quad \min_{\underset{\sim}{\delta}} \underset{\sim}{g}_o (\underset{\sim}{\varepsilon}) \qquad (10)$$

An iterative gradient solution is required and estimates are unbiased in the presence of both measurement and process noise when a maximum likelihood minimisation scheme is used.

Referring to Fig 4, it can be seen that the user has the option of conducting model structure and parameter estimation in the time or frequency domain; for helicopter applications there are many advantages in the frequency domain approach, providing of course that linearity assumptions hold. Higher order dynamic effects can result in the corruption of quasi-steady parameters estimated in time domain models. Another problem that often arises stems from the correlation or linear dependence of information in different elements of the state vector or aircraft motion; with weakly damped modes, helicopters are particularly prone to this problem when a badly designed test input leaves a strong residue in the free response. A method for maximising confidence in parameter estimates in such cases involves transforming to a new set of state variables, when the offending dimensions with little information content can be excluded. The effects of frequency and number of dimensions (orthogonal components) on the confidence in the estimation of the pitch damping derivative M_q is shown in Fig 5. The higher the

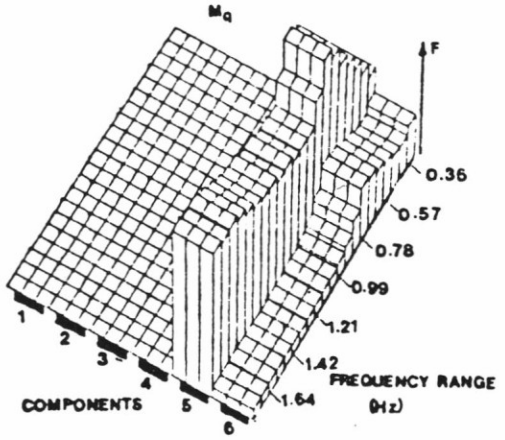

Fig 5 Variation of partial F-ratio for M_q with frequency range and number of orthogonal components

F-ratio[5], the lower the parameter standard deviation and Fig 5 shows how a frequency range of about 0.5 Hz and excluding one of the orthogonal components gives the highest confidence in M_q. These rank-deficient solutions and truncation in the frequency domain are elements of the integrated system identification toolkit necessary for helicopter applications. Examples of their use will be presented in the next Chapter.

3 HELICOPTER FLIGHT DYNAMICS - 3 EXAMPLES

The examples highlighted in this Chapter cover lateral/directional motions, longitudinal short period dynamics in forward flight and vertical axis dynamics in the hover. In all three cases the flight test data presented are derived from experiments with the RAE research Puma (Fig 6) and the simulation results from Helistab. The

Fig 6 RAE(Bedford) Research Puma

examples are selected to illustrate areas where approximate formulations are valid or where modelling expansions in both nonlinearity and dynamic range are required. The examples will also illustrate that the level of modelling adequate for describing and predicting a broad class of problems is far from uniform. Local analytical approximations, valid over a very limited range of conditions, are often required to derive insight into causal physical mechanisms.

3.1 Lateral-directional dynamics

The variation of Dutch-roll stability with flight path angle can be quite marked in helicopters, often precluding certification for climb-out flight phases without significant autostabilisation. The Puma is typical and pedal doublet responses for descent, level and climb conditions are shown in Fig 7; the Dutch-roll oscillation is moderately damped in descent, close to neutral in level flight and divergent in the climb. Previous work[9] has highlighted the importance of couplings with longitudinal and rotor motions on this oscillatory mode, but some insight can be gleaned as to the primary physical effects from examination of simple lateral/directional dynamics. Two important parameters are the 'weathercock' and dihedral effects on yawing and rolling moments with respect to sideslip, N_v and L_v. Fig 8 shows the variation of these parameters with flight path angle, predicted from theory and estimated from flight test data. Noticeable features are the much lower N_v values predicted by Helistab and the much stronger increase in dihedral effect in the climb estimated in flight. Both of these comparisons will lead to poor correlation between flight and theory. Using flight estimated derivatives[10] for the remaining elements of the lateral/directional sub-system, a comparison of Dutch-roll eigenvalues (Table 2) indicates that both the period and the damping are poorly predicted by theory.

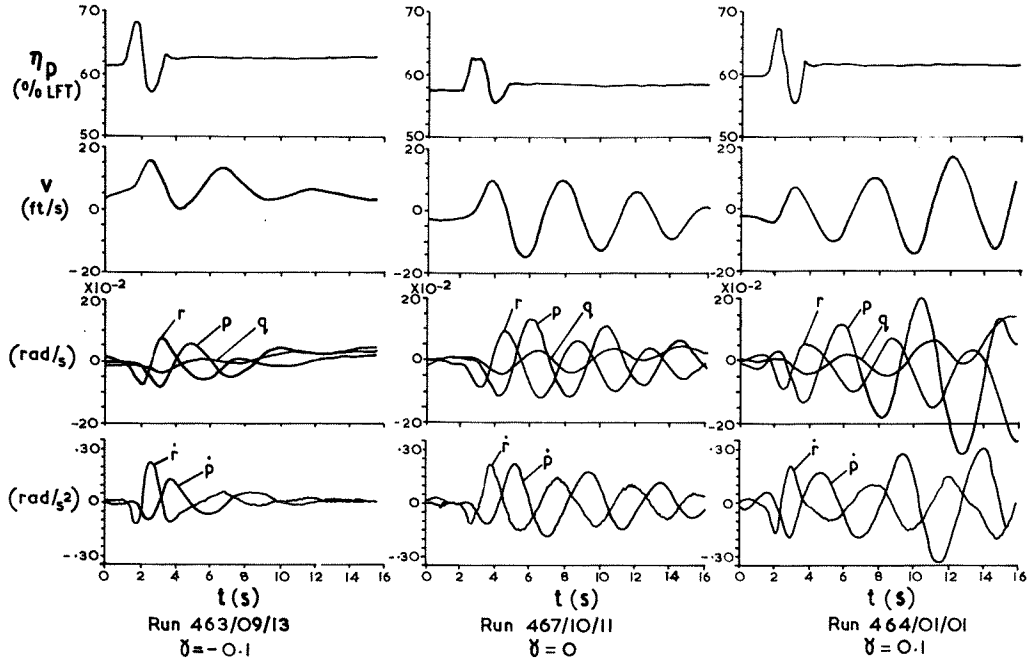

Fig 7 Puma response to pedal doublet (100 kn-descent, level, climb)

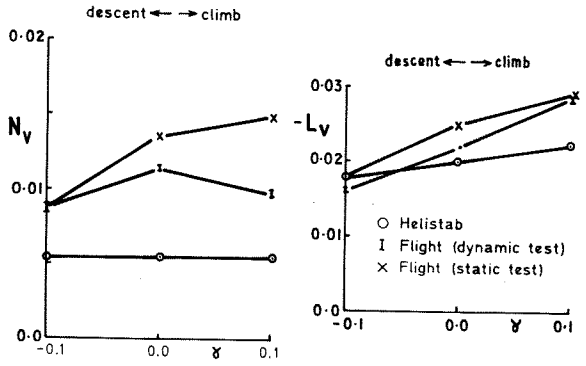

Fig 8 Variation of weathercock (N_v) and dihedral (L_v) effects with flight path angle - Puma, 100 kn

Table 2

DUTCH-ROLL EIGENVALUE VARIATION

	Helistab	Flight Estimates
Descent	$-0.106 \pm 0.9i$	$-0.17 \pm 1.37i$
Level	$-0.057 \pm 0.94i$	$-0.118 \pm 1.53i$
Climb	$-0.037 \pm 0.94i$	$0.052 \pm 1.45i$

The low values of N_v derived from the simulation model can be attributed to a relatively strong nonlinear variation of yawing moment with sideslip angle[9], caused by the large thickness-to-chord ratio of the vertical stabiliser and the interaction with the main rotor wake. The simulation values shown in Fig 8 were derived from a small-perturbation differencing technique. Increasing the perturbation size to values closer to those experienced in the flight data shown in Fig 7, leads to a corresponding increase in weathercock stability to within 20% of flight values. The powerful dihedral effect estimated in the climb condition will have a strong effect on Dutch-roll damping only in the presence of adverse yaw (N_p) . For the Puma, a high value of the product of inertia I_{xz} leads to such a high adverse N_p through roll/yaw coupling. An approximation for the Dutch-roll damping can then be written in the form,

$$(2\zeta\omega)_{\text{Dutch-roll}} = -\left(N_r + N_p \frac{VL_v}{L_{\dot{p}}}\right) \qquad (11)$$

The post-multiplier of N_p in equation (11) compares well with the roll/yaw ratio across the flight path angle range under study[10], confirming the destabilising effect of dihedral. A comparison of original and 'upgraded' Helistab (linearised) model responses with flight data is shown in Fig 9, illustrating the improvements in damping and frequency predictions. A simple 4th order lateral/directional model was sufficient to explain the principal features of the dynamic motion, although the presence of strong non-linearities in the yawing moment demonstrates the

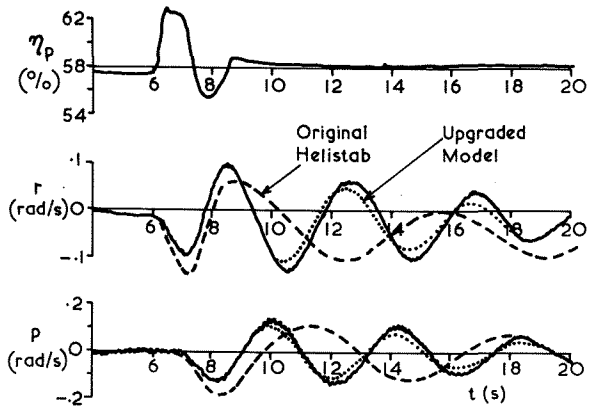

Fig 9 Comparison of original and upgraded Helistab models

importance of using the full nonlinear simulation model for more general handling studies. The origin of the 40% increase in dihedral in the climb condition remains something of a mystery at this level of modelling.

3.2 Short-period pitch dynamics

The character of the short term response to pilot pitch control inputs is strongly configuration dependent, with the stiffness and Lock numbers (λ_β , γ) having marked effects on pitching moment derivatives. This is true to the extent that the short-period approximation is only valid for use over a limited configuration and flight condition range. Fig 10 illustrates the point showing the variation of longitudinal 'short-period' eigenvalues with speed for two configurations ($\lambda_\beta{}^2$ = 1.06, 1.27) spanning the range of current operational types. The approximations shown are derived from the roots of the quadratic

$$\lambda^2 + (2\zeta\omega)_{sp}\lambda + \omega_{sp}^2 = 0 \qquad (12)$$

where

$$(2\zeta\omega)_{sp} = -(Z_w + M_q) \; ; \qquad (13)$$

$$\omega_{sp}{}^2 = Z_w M_q - M_w V \qquad (14)$$

Whereas a normal short-period oscillation exists for the longitudinal (2 degree of freedom) approximation for the softer rotor, the stiff configuration exhibits an aperiodic divergence at high speed. Coupling with lateral motion destroys the oscillatory character present in the soft rotor modes. For the stiffer rotor the unstable divergence at high speed is captured by the simple 2 degree of freedom approximation.

Understanding the short term pitch response of helicopters through derivative-type models is again limited by bandwidth and non-linearity. Fig 11 shows the response of the Puma to a cyclic doublet input at 100 kn, compared with the Helistab responses. A time shift, longer term departure and weak roll correlation are notable features of the comparison. Ref 5 discusses the

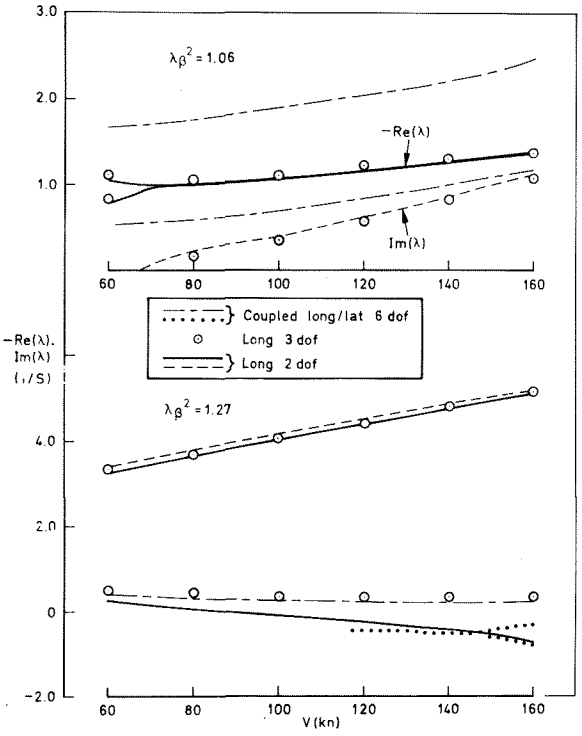

Fig 10 Variation of exact and approximate longitudinal short-period eigenvalues with speed

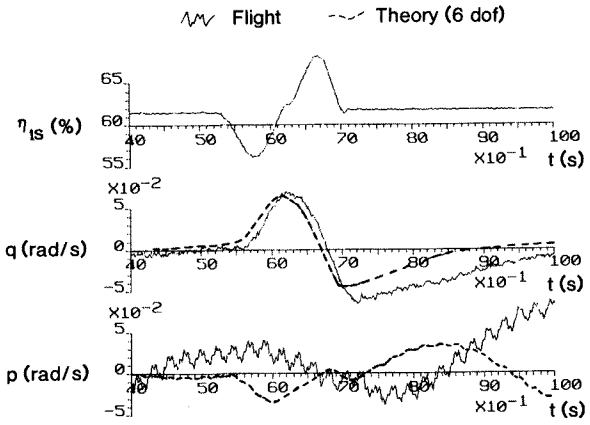

Fig 11 Puma response to F/A cyclic doublet at 100 kn

estimation of the full range of pitch derivatives from this response but Fig 12 draws particular attention to the estimation of pitch damping M_q . Estimates from five methods are shown normalised by the theoretical value. The rank-deficient estimate (see Fig 5) shows some improvement over the basic equation-error regression method, but using this to initiate the output-error method hardly changes the resulting converged estimates.

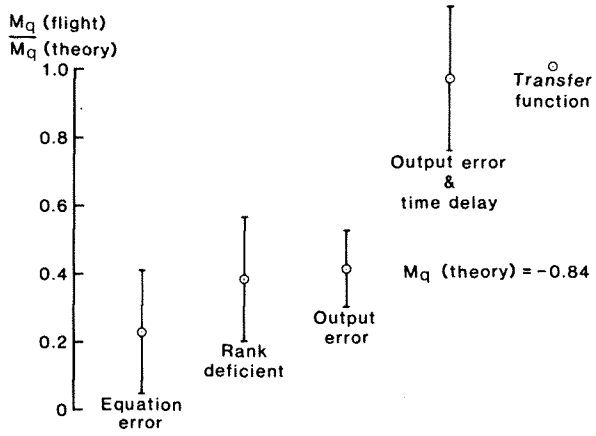

Fig 12 Pitch damping estimates from flight - Puma cyclic doublet, 100 kn

Only when a time delay between control input and aircraft response is incorporated in the estimation scheme does the value come close to the Helistab prediction and even then with a standard error of some 20%. The transfer function model estimate is also shown on Fig 12 and Table 3 shows how the short period parameters compare with theory (cf equation (12)).

Table 3

PITCH SHORT PERIOD OSCILLATION PARAMETERS

Parameter	Estimate	1σ Error Bound	HELISTAB
ω_{sp}^2	0.877	0.45	0.93
$2\zeta\omega_{sp}$	1.655	0.29	1.76
$M_{\eta 1s}$	-0.0407	0.007	-0.0376
$Z_{\eta 1s}$	3.69	1.63	0.618
τ_θ	0.195	0.08	-

Also shown in Table 3 are estimates of the control derivatives $M_{\eta 1s}$, $Z_{\eta 1s}$, but the magnitude of the estimated pure time delay τ_θ is the most striking feature. This is a characteristic result of 6 degree of freedom estimation in helicopters whereby good estimates of damping can only be achieved by introducing a delay artefact. Part of the problem lies in the exclusion of higher order rotor dynamics: Fig 13 shows the response of the 3 degree-of-freedom tip-path-plane dynamic model. The time delay has now virtually disappeared. Also shown in Fig 13 is a comparison of the rotor disc flapping motions β_{1c} , β_{1s} and coning β_o . The flight measurements were derived from blade flapping sensors converted to multi-blade coordinates. The correlation of longitudinal flapping and coning is very good, indicating a high confidence in this form of rotor modelling, at least for small perturbations about a trim condition.

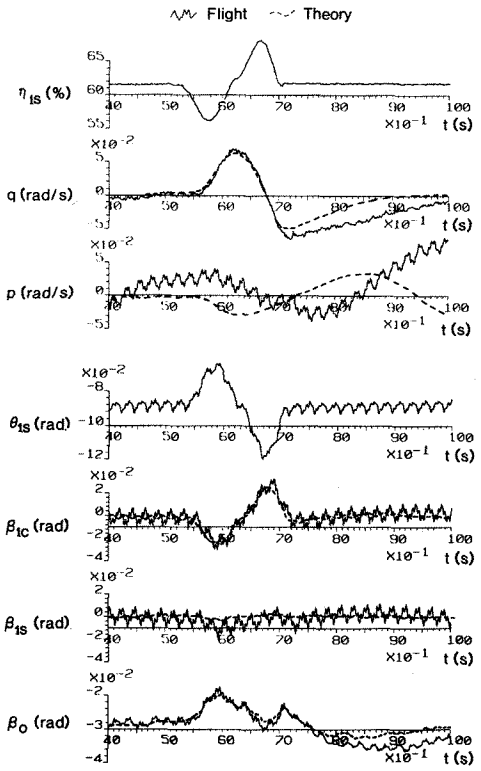

Fig 13 Puma response to F/A cyclic doublet at 100 kn

This example has provided some insight into the value of reduced order modelling of helicopter pitching motions. True causal modelling requires expanding the model structure to include rotor dynamic effects and this is known to become even more important at higher frequencies[11]. Perhaps the only satisfactory way forward in these cases is to conduct identification on the expanded model structure and include such parameters as Lock number and flap frequency as unknowns within the estimation scheme. Preliminary results in this area[12] are already very encouraging, indicating that using the more detailed measurements leads to, in some cases, very high confidence in estimates of fundamental rotor parameters.

3.3 Vertical axis dynamics in hover

Modelling helicopter behaviour in hover or vertical climb, with the rotor operating in axial flow conditions, appears, at least on the surface, to be a relatively straightforward problem. The use of momentum theory in this context is well established and the rotor thrust T developed by an actuator disc, in the steady state, takes the form

$$T = \rho(\Omega R)^2 \pi R^2 \lambda_o(\lambda_o - \mu_z) \qquad (15)$$

where λ_o is the uniform downwash, μ_z the normal velocity (both normalised by the tip-speed ΩR) and R the blade radius. Combining

equation (15) with simple 2-D blade element theory gives the first order formulation for vertical axis dynamics, in terms of the vertical velocity w and rotor collective pitch θ_o ,

$$\dot{w} - Z_w w = Z_{\theta_o} \theta_o \qquad (16)$$

where

$$Z_w \text{ (heave damping)} = -\frac{\rho a_o \sigma (\Omega R)}{8(m/\pi R^2)(1 + a_o\sigma/16\lambda_o)} \qquad (17)$$

$$Z_{\theta_o} \text{ (control sensitivity)} = -\frac{4}{3}\Omega R Z_w$$

m is the aircraft mass, and σ the rotor solidity. This first order model has formed the basis for handling criteria and simulation modelling for a wide range of applications. However, for aggressive height keeping where short term response becomes important, there is strong evidence to indicate that this model is quite inadequate. Fig 14 illustrates a comparison between flight test and theory for the normal acceleration

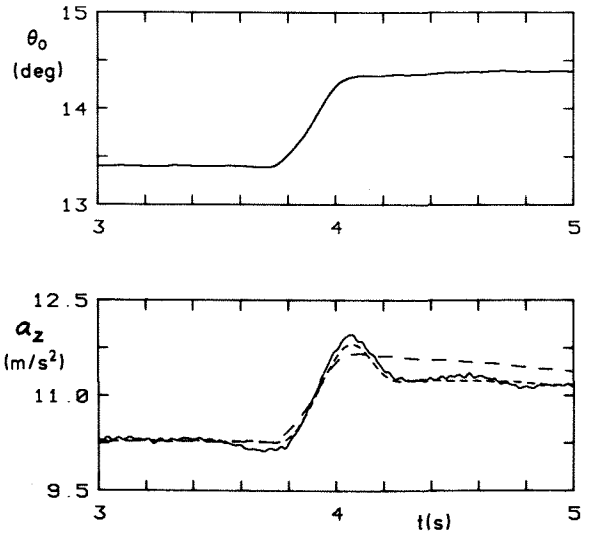

Fig 14 Puma normal acceleration response to step collective input in hover;
—— flight,
– – 1 degree of freedom (Helistab),
--- 3 degree of freedom identified model

response to a step collective input. The long-broken line gives the Helistab result, completely missing the initial overshoot and predicting a slightly stronger decay. Identification of equivalent damping and control sensitivity from flight data typically produces estimates of the order of 50% of the values given by equation (17). Expanding the model structure to include both rotor coning and dynamic inflow, as in equation (10) provides a much better comparison with theory and can serve to explain the anomalies in the equivalent parameters. Recently, these modelling enhancements have been the subject of debate[13,14] in the literature; the results in this paper are taken from Houston's work at the RAE[15]. A frequency sweep test technique has been designed to excite the aircraft over a suitable bandwidth and to provide measurements for transfer function identification. Fig 15 shows results for the normal acceleration to collective gain, phase and coherence up to about 3.5 Hz. The broken line shows the best fit for a 4th order model structure, consistent with the inclusion of 2nd order rotor coning and 1st order inflow; both normal acceleration and coning measurements were used to derive the least-squares fit, which is very good over a wide frequency range. The model structure given by equation (16), in contrast, would of course produce a constant gain with frequency.

The parameters from the transfer function model can be converted to a consistent state space model and compared with theoretical predictions. The new parameter set is now a more fundamental one of blade properties, given in Table 4.

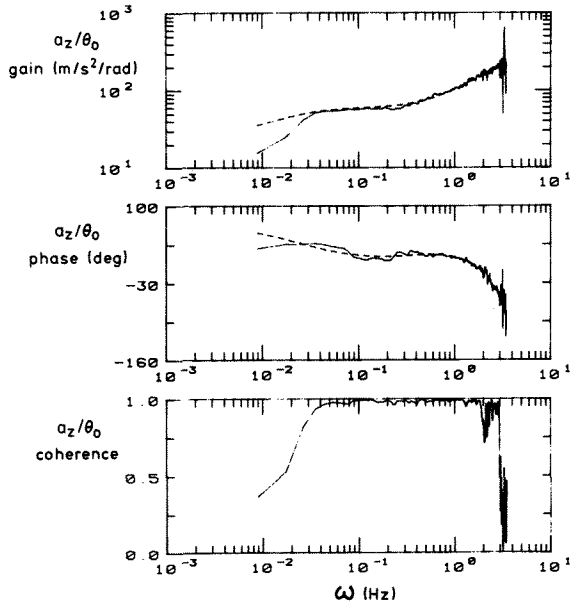

Fig 15 Normal acceleration-collective pitch transfer function, Puma hover;
—— flight,
--- 3 degree of freedom heave/coning/inflow model

Here m_β is the blade first moment of mass and C_o the coefficient of apparent mass in the unsteady momentum theory[14]. The comparisons raise several interesting questions regarding the blade mass distribution, aerodynamic efficiency and adequacy of the dynamic inflow model used. These are addressed in more detail in Ref 15, but Fig 14 shows, as the short-broken line, the response of the derived 3 degree of freedom model to the step input; the coning response gives a similar

Table 4

COMPARISON OF ESTIMATED AND PREDICTED ROTOR PARAMETERS - PUMA HOVER

Rotor Parameter	Flight Estimate	Theory
a_o	5.79	5.73
λ_o	0.053	0.054
γ	7.8	8.56
m_β	308	275
C_o	0.64	0.64

agreement and this is strong evidence that this level of modelling is satisfactory for short term vertical axis response. The goodness of fit in Fig 15 suggests that the range of validity of the model could be extended to much higher bandwidth.

As a final note on vertical axis response, Ref 15 presents results for the primary and coupling components of the quasi-steady derivative Z_w , reduced from the third order form via the mechanism shown in equation (6). Writing this in the form,

$$Z_w = Z_w^* + \delta Z_w \qquad (18)$$

where the δ term represents the weak coupling from the inflow and coning degrees of freedom, Table 5 shows a comparison of results.

Table 5

COMPARISON OF VERTICAL AXIS DAMPING FROM THEORY AND FLIGHT

	Flight Test	Theory
Z_w^*	0.09	0.09
δZ_w	-0.26	-0.41
Z_w	-0.17	-0.32

Perhaps the most striking difference revealed by Table 5 is in the coupling terms, and these go a long way to explaining the origin of the low flight estimates, compared with theory. Ref 15 identifies a major source of the anomaly to be the modelling of inflow damping. Momentum theory is a gross simplification of real effects here of course, and it is likely that a more detailed level of modelling is required to maintain a uniform validity from initial control input to steady state normal velocity. This is an area for future research.

4 TOWARDS LEVEL 2 MODELLING

The special features that make Level 1 models so amenable to analysis - rigid blades and linear integrated loads are, of course, the very source of their limitations. They preclude an accurate prediction of a wide range of problems including the bandwidth constraints on high gain active control systems, dynamic loads at the safe flight envelope boundary and numerous operational aspects that impact on flying qualities, eg penetration effects from strong atmospheric disturbances, rotor-blade icing etc. Modelling features that offer the level of detail to enable a treatment of these effects have been discussed in Chapter 2 of this paper; the rotor system represents the most significant element and the features that distinguish Level 2 modelling are unsteady, non-linear aerodynamics on the one hand and a coupled modal description of the elastic deformation on the other. These are features commonly found in Level 3 (Table 1) rotor loads/vibration analyses where a quite different set of design rules and parameter sensitivity functions apply than in flight dynamics. For the latter, such rules are still very immature if they exist at all, and fundamental research is still required to map these into Level 2 model structures. This is the aim of an integrated research programme in the UK, combining the RAE Bedford resources with those in Universities, notably Bristol (aeroelastic modelling), Glasgow (system identification validation tools) and Cranfield (unsteady aerodynamics). These activities will be reported on future occasions as the programme develops, but in this paper some results are presented of the kind of flight measurements required to support validation. Blade deformations and aerodynamic loads can be approximately derived from carefully distributed surface pressure sensors and strain gauges. Table 7 summarises the steps required in the analysis, and in an RAE developed estimation software package (RIBAN).

Table 7

RESEARCH INSTRUMENTED BLADE ANALYSIS (RIBAN) FOR AEROELASTIC MODELLING

MEASUREMENTS
Distribution of surface pressures and strains
ANALYSIS
Reduce C_{ple} to α and C_N (using 2-D test database)
Reduce strains to displacements and loads (strain pattern analysis)
Compute local incidence components
Compute spatial/temporal inflow distribution
Conduct C_N , inflow and loads modelling validation

The leading edge (2%c) pressure transducer is the key sensor whose measurement, using a 2-D test (unsteady) calibration database, can be transformed into blade incidence and normal force coefficient. The trailing edge sensor is essentially a stall indicating sensor, necessary since the unique relationship between the leading edge pressure measurement and incidence breaks down above stall (Fig 16). This incidence measuring

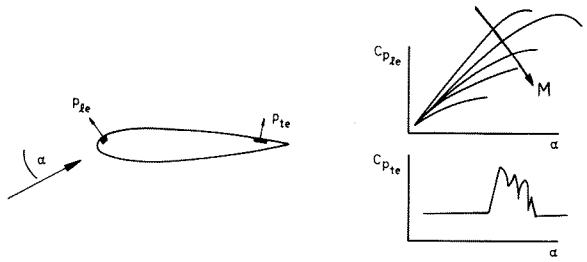

Fig 16 Surface pressure sensors as incidence and stall indicators

technique has been developed at RAE (Ref 16), as has the strain pattern analysis technique (Ref 17), to derive an equivalent displacement pattern from the strain measurements based on a set of measured calibration modes.

Details of these techniques can be found in the References and Table 7 indicates the relevant analysis stages - from local blade incidence computation to loads and inflow model validation. At RAE Bedford, the research Puma is currently fitted with experimental Research Instrumented Blades (RIBs) with pressure and strain sensors distributed as shown in Fig 17; the proposed layout for the research Lynx RIBs is also shown.

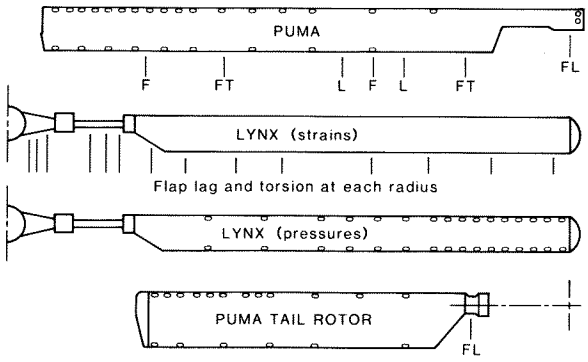

Fig 17 Sensor distributions for Puma and Lynx RIBs

The kind of measurements described above holds the key to the development and validation of new inflow representations that correctly predict incidence changes in manoeuvring flight and the dynamic effects of blade stall induced by blade/vortex interaction. Wake models, even in prescribed form, are still too time consuming even on super-computers for real-time simulation, and rational approximations for dynamic inflow models valid across a wide range of conditions are required. Even in steady flight, however, incidence variations are difficult to predict in detail. Fig 18 shows a comparison of simple theoretical (Level 1) incidence contours (uniform and linear longitudinal variation of inflow) with flight measurements derived from the Puma RIB at about 100 kn and modest thrust coefficient. The fine detail in the flight results reveals considerably more azimuthal variations than predicted

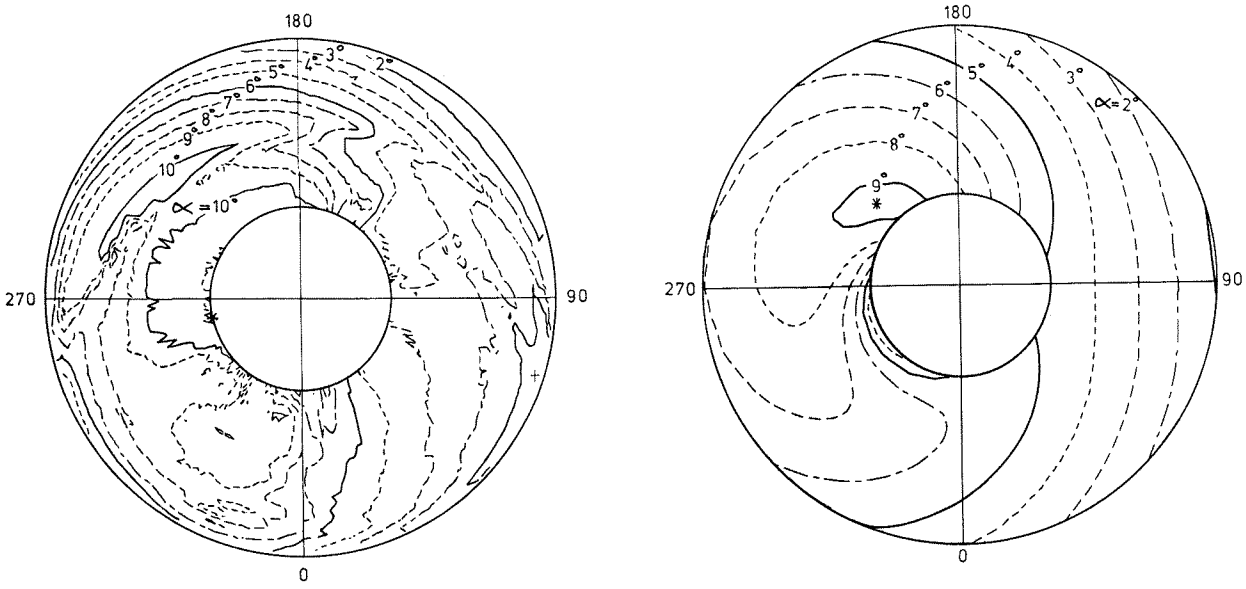

Flight Helistab

Fig 18 Incidence contours - Puma, 100 kn

(numbers on lines refer to local incidence in degrees)

by simple theory. The high incidence cell on the retreating side has moved outboard and there is considerably more 'texture' around the advancing side. In manoeuvres, a two-time scale assumption provides a mechanism to interpret quasi-steady variations of induced incidence harmonic components, ie independently of the azimuthal time scale. This is the basis of current research at RAE to extend existing generic (momentum) theories and will be covered in future publications.

The extent of the modelling enhancements in both bandwidth and nonlinearity at Level 2, to provide complete confidence in predictions through the design-certification life cycle, is still an area of research as noted above. The price of increased fidelity, however, is likely to be an increased difficulty in relating cause and effect through the multi-path, multi-parameter model. Recognising this kind of problem highlights the need for the continuing research into rational analytic approximations in helicopter flight dynamics and extending the Level 1 practices, as typified by the examples in this paper, into the Level 2 régime. The need for new initiatives in this area could be as pressing as the need for increased processing speed to provide a real-time capability. Physical insight can be hard to find within the behaviour of a nonlinear, non-stationary system, and it is likely that good approximations will have only a limited range of application, conditioned by the particular problem being tackled. Although restricted, the theoretical reinforcement that narrow range approximations give to understanding general trends on the one hand and limiting cases on the other, can be invaluable.

5 CONCLUSIONS

The analysis of helicopter flight dynamics requires a comprehensive nonlinear simulation model, validated fit for predictive use throughout and beyond the design envelope. In addition, a set of rational approximations derived from reduced order models, is required to gain physical insight and to establish important trends and parameter effects. This paper has described how theoretical model structures can be built up of elements of increasing complexity based on the natural modelling dimensions of frequency and amplitude. Three roughly defined modelling levels are suggested; Level 1 contains most of the current flight dynamics modelling assumptions while Level 3 pertains more to rotor load predictions over a wide bandwidth. The need for increased fidelity in flight dynamics simulation models, at Level 2, has been discussed. Validation methodology has been addressed within the framework of system identification techniques. Examples have been presented, largely from Level 1 model structures, of how theoretical predictions compare with actual flight behaviour. From the general issues discussed and the special examples given, a number of important observations and conclusions can be drawn.

(1) Model development and validation need to proceed hand-in-hand, with flight measurements compatible with model complexity.

(2) The greater the demand on simulation fidelity (through increased model complexity), the greater the need for authentic cause and effect rational approximation theory.

(3) System identification offers a systematic procedure for conducting validation studies through model structure and parameter estimation. The methodology is approaching a level of maturity where it can be used routinely for flight test data analysis.

(4) Stability and response characteristics of helicopters can be significantly affected by model structures even within the Level 1 framework, eg:

- variations in Dutch-roll stability with flight-path angle, dependent on non-linear behaviour and roll/yaw coupling,
- short-period pitch dynamics affected by lateral couplings and tip path plane dynamics,
- heave response in the hover matched by a model structure including rotor coning and inflow dynamics.

(5) Flight measurements of rotor incidence distributions using a simple set of surface pressure and static sensors will form the basis for Level 2 model validation at RAE Bedford.

(6) Research is required to establish the extent to which rotor modes, unsteady aerodynamic effects and other non-rotor modelling developments need to be included in Level 2 models to ensure high predictive quality for new flight dynamics design rules.

Significant reduction in certification timescales and costs and high confidence levels in design prediction are worthy goals to stimulate an increasing investment in helicopter flight dynamics modelling capability. It is the author's view that they will certainly not be achieved unless equal attention is given to the development of validation techniques coupled with narrow range approximation theory.

ACKNOWLEDGMENTS

The author is grateful to colleagues for the contributions made to this paper; to Stewart Houston and Jane Smith of RAE Bedford for the vertical axis results in section 3.3 and the incidence contours in section 4 respectively, and to Colin Black at Glasgow University for the maximum likelihood and rank-deficient estimates of M_q in section 3.2.

REFERENCES

1 T. Wilcock, Ann C. Thorpe, 'Flight simulation of a Wessex helicopter - a validation exercise', RAE Technical Report 73096, (1973).

2 G.D. Padfield, 'A theoretical model of helicopter flight mechanics for application to piloted simulation', RAE Technical Report 81048, (1981).

3 B.N. Tomlinson, G.D. Padfield, 'Piloted simulation studies of helicopter agility', Vertica, Vol 4, pp. 79-106, (1980).

4 G.D. Padfield et al, 'UK research into system identification for helicopter flight mechanics', Vertica, Vol 11, pp. 665-684, (1987).

5 C.G. Black, D.J. Murray-Smith, G.D. Padfield, 'Experience with frequency domain methods in helicopter system identification', Paper No 76, 12th European Rotorcraft Forum, Garmisch - Partenkirchen, FRG, September 1986.

6 W. Johnson, 'Helicopter theory', Princeton University Press, Princeton, (1980).

7 R.D. Milne, 'The analysis of weakly coupled dynamical systems', Int. J. Control 2, No 2, (1965).

8 G.D. Padfield, 'On the use of approximate models in helicopter flight mechanics', Vertica, Vol 15, pp. 243-259, (1981).

9 G.D. Padfield, R.W. DuVal, 'Application of system identification to the prediction of helicopter stability, control and handling characteristics', Helicopter Handling Qualities, NASA CP-2219, April (1982).

10 G.D. Padfield, 'Integrated system identification methodology for helicopter flight dynamics', Proceedings of the 42nd Annual Forum of the American Helicopter Society, Washington DC, June (1986).

11 R.T.N. Chen, M.B. Tischler, 'The role of modelling and flight testing in rotorcraft parameter identification', Proceedings of the 42nd American Helicopter Society Forum, Washington DC, June (1986).

12 Proceedings of the TTCP workshop on 'The identification of rotor flapping dynamics', held at RAE Bedford April 21-25, 1988, (unpublished).

13 R.A. Feik et al, 'Validation of a mathematical model of a Sea King Mk 50 helicopter using flight trials data', Paper No 7.5, Proceedings of the 14th European Rotorcraft Forum, Arles, France, September (1987).

14 R.T.N. Chen, W.S. Hindson, 'Influence of dynamic inflow on the helicopter vertical response', Vertica, Vol 11, No 1/2, pp. 77-91, 1987.

15 S.S. Houston 'Identification of factors influencing rotorcraft heave axis damping and control sensitivity in the hover', RAE Technical Report (in preparation), 1988.

16 P. Brotherhood, 'An appraisal of rotor blade-tip vortex interaction and wake geometry from flight measurements', AGARD CP 334 - Prediction of aerodynamic loads on rotorcraft, September 1982, (also RAE Technical Memorandum FS(B) 461, February (1982)).

17 A.R. Walker, 'Comparison between theoretically and experimentally derived vibration mode shapes of a rotating model helicopter blade', RAE Technical Report 82056 (1982).